

EXPERIMENTAL AND ANALYTICAL STUDY ON HIGH-PERFORMANCE BUCKLING RESTRAINED BRACE DAMPERS FOR BRIDGE ENGINEERING

Tsutomu Usami¹, Hanbin Ge¹ and Xiao-Qun Luo²

ABSTRACT

This paper presents performance requirements of high performance dampers for the damage control seismic design of steel bridges. To verify the proposals, an idea of high-performance buckling restrained braces is proposed that is expected to withstand major earthquakes three times without being replaced. A series of performance tests and analyses are carried out to clarify the required demands. It has been shown that installing BRBs is one of the most efficient ways to control seismic damage in steel bridges.

INTRODUCTION

In recent years, seismic damping devices are widely used in damage control design for bridge engineering as well as building engineering. Based on the design philosophy, damage is expected to concentrate in damping devices during severe earthquake, and correspondingly damage of main structures can be controlled. Among many types of damping devices, hysteretic dampers have been caught more and more attractions because the inelastic deformation capability of metallic substances represents an effective energy absorption mechanism for damping of engineering structures with low cost (Weber et al. 2006).

According to the yield mechanism, hysteretic dampers are divided into axial-type, shear-type, bending-type and torsion-type. So far, as an axial-type damping device, buckling restrained braces (BRBs) are widely studied on component behaviours and system applications in building (Iwata et al, 2006; Fahnestock et al., 2007) and bridge engineering (Usami et al., 2005). As an instance on component level, ductility capacity models for BRBs are developed to predict the cumulative plastic ductility capacity (Andrews et al. 2009). Moreover, improved types of BRBs are in development, such as double steel cores encased in twin steel tubes and infill concrete tested by Lai and Tsai (2004). Besides test and analysis researches on component level, more investigations were conducted on systems under cyclic loadings. A series of experimental and analytical studies were conducted by Uriz and Mahin (2008) to improve understanding of the behaviour of concentrically braced frames including buckling-restrained braced frames under cyclic inelastic deformations. As an example in bridge engineering, buckling restrained braced ductile end cross frames were proposed for steel plate girder bridges with different end connections to upgrade effectiveness of seismic damage control (Carden et al. 2006). The ductile end diaphragm with BRB end diaphragms were introduced in regular slab-on-girder or deck truss steel bridges to make it applicable in bidirectional earthquake excitations (Celik and Bruneau 2009). It has been found from recent research series by the authors that light weight BRBs were employed to replace insufficient lateral braces and cross diagonal braces for retrofitting an

¹ Professor, Dept. of Civil Engineering, Meijo University, Nagoya, Japan

² P.D. Researcher, Advanced Research Center for Seismic Experiments and Computations, Meijo University, Japan

existing steel arch bridge, which leads to damage concentration in sacrificing damping devices and mitigates damage of main structures (Usami et al., 2005, 2008, 2009).

A high performance seismic damper (i.e., HPSD) is the damping device that no replacement is needed during the lifecycle of bridges and it is likely to suffer 3 times of strong earthquake without severe damage. Here, based on authors' past research, performance tests and analyses are carried out to develop new BRBs to meet the requirement of high performance damping devices, and as a result, a design guideline for application of the dampers has been proposed.

PERFORMANCE REQUIREMENT OF HIGH-PERFORMANCE SEISMIC DAMPERS

Compared to seismic dampers in building engineering, disadvantages exist in seismic dampers in bridge engineering, such as large-scale or suffering more rigorous environment (e.g. long term wind and rain). Therefore, besides general performance requirements for seismic dampers in building engineering, additional special performances for seismic dampers in bridge engineering are requested. Performance requirements for high-performance seismic dampers in bridge engineering are summarized as follows (Usami, 2007):

- (1) Stable hysteretic characteristics and high energy absorption capacity;
- (2) High deformation capacity;
- (3) High low-cycle fatigue strength;
- (4) High durability;
- (5) Easy fabrication and construction, low cost;
- (6) No need of replacement.

In the performance based safety verification method, two performance indices, i.e., deformation and low cyclic fatigue can be employed to quantify the requirement. For level 2 earthquakes, the deformation capacity should satisfy such an inequality as follows:

$$\gamma \cdot \varepsilon_{\max} \leq \varepsilon_u = 0.3 \quad (1)$$

and in the verification of low cycle fatigue, cumulative inelastic strain should satisfy:

$$CID = \gamma \cdot n \sum_{i=1}^n |\varepsilon_{pi}| \leq CID)_{\lim} = 0.7 \quad (2)$$

where, ε_{\max} = maximum value of average strain response; ε_u = ultimate strain; γ = partial factor; CID = cumulative inelastic deformation; ε_{pi} = plastic component of average strain response; $CID)_{\lim}$ = limit value of cumulative inelastic deformation.

In the paper, the examination of item (1) is the main content of the above mentioned requirements and spindle shaped hysteretic curves induced by strength deterioration must be prevented in hysteretic seismic dampers under cyclic loadings. Details are mentioned in the following sections. The examination of items (2) and (3) is carried out through Eqs.(1) and (2) in which larger ultimate strain ε_u and CID are given to satisfy the high performance requirement. To guarantee the item (4), steel corrosion should be avoided. And for items (5) and (6), it is thought that the use of steel is economic and easy to reach the target.

Hereinafter, with relation to performance requirements of high performance dampers, high performance BRBs is discussed in detail. Experimental investigations of light weight high performance BRBs are carried out. An elasto-plastic model for simulation of BRBs is proposed and numerical analyses are performed to compare with the results of experiments.

BUCKLING RESTRAINED BRACE (BRB)

Overall buckling prevention condition equation of BRBs

Because BRBs in bridge engineering are generally in large-scale, the influence of initial deflection by self-weight grows and the construction of BRBs becomes difficult, so developing light-weight seismic dampers is needed. Consequently, to ensure high performance of BRBs, overall buckling should be carefully examined to satisfy the requirement of item 1) mentioned in section 2.

For BRBs with simply supports at both ends, the general condition equation to prevent overall buckling in BRBs is expressed as follows:

$$\frac{P_{\max}(a+d+e)}{1 - \frac{P_{\max}}{P_E^R}} \leq M_y^R \quad (3)$$

where, M_y^R = yield moment of the restraining member; P_{\max} = maximum compression force of the brace member; P_E^R = the Euler buckling load of the restraining member; a = maximum initial deflection at the mid-span of the restraining member; d = gap width between the restraining member and the brace member; e = eccentricity of axial load (assuming equal in both ends). The left side of the equation is the bending moment including $P-\Delta$ effect at the mid-span of the restraining member, and the right side is the yield bending strength of the restraining member, which is assumed as limit state.

Solving Eq. (3) at the limit state, P_{\max} can be obtained as follows:

$$v_F = \frac{P_{\max}}{P_y} = \frac{1}{\frac{P_y}{P_E^R} + \left(\frac{P_y L}{M_y^R}\right) \cdot \frac{a+d+e}{L}} \quad (4)$$

Here, P_y = yield axial compression force of the brace member. A nominal safety factor v_F is defined in Eq. (4) as the ratio of maximum axial compression force to yield axial force at the limit state when overall buckling occurs in the BRB. Before the application of Eq. (4), the maximum axial compression load, P_{\max} , is predicted by assuming variables in Eq. (4) that nominal values of material constants, design values of geometric dimension and initial deflection of $a=L/1000$ are used; other uncertain factors such as variations of initial deflection, gap width and eccentricity are considered as a decline rate of $1.0/f(U.F.)$ at the right side of the equation.

Moving the ratio to the left side, a safety factor of 3.0 is proposed as follows:

$$\frac{P_{\max}}{P_y} \cdot f(U.F.) = \frac{P_{\max}}{P_{y)actual}} \cdot \frac{P_{y)actual}}{P_{y)nominal}} \cdot f(U.F.) = 3.0 \quad (5)$$

where, $P_{\max}/P_{y)actual}$ is the ratio of the maximum axial compression load to the actual yield axial load and it is about 1.6; $P_{y)actual}/P_{y)nominal}$ is the ratio of the actual axial compression load to the nominal yield axial force and it is about 1.2; the value of $f(U.F.)$ is about 1.56. Thus the condition equation to prevent overall buckling in BRBs can be expressed as follows:

$$v_F = \frac{1}{\frac{P_y}{P_E^R} + \left(\frac{P_y L}{M_y^R} \right) \cdot \frac{a + d + e}{L}} \Bigg)_{nominal} \geq 3.0 \quad (6)$$

Tests of BRBs

As shown in Fig. 1, the light-weight high performance BRB is made up of a steel plate brace member, a pair of T shaped steel restraining members connected by bolts and un-bonded material stuck to the brace member. In the study, cyclic loading tests on five specimens were carried out to investigate BRBs' behavior. The geometric dimension variables in specimens include dimensions of the restraining member and the gap width between the brace member and the restraining member. Geometric dimensions and material constants of specimens are listed in Tables 1-3.

Specimens

(1) Brace member

The full view of the brace member is shown in Fig. 1(a), geometric dimensions and structural properties are listed in Table 1. A flat steel plate is used as the brace member, and to connect to experiment equipments well, cruciform sections at both ends are expanded by welding 12mm thick rib stiffeners to both side of the plate. SM400A mild steel was used for the brace member. Three JIS No.1-typed test pieces are made from the same steel of the brace member and average values tested are taken as material constants listed in Table 2.

Table 1 Geometric dimensions and structural properties of brace members

Specimens	Steel	L (mm)	B (mm)	t (mm)	A (mm ²)	λ	P_y (kN)	δ_y (mm)
B1	SM400A	1355	100	10.3	1030	454	280	1.73
B2				10.4	1040	450	283	
B3				10.3	1030	454	280	
B4				10.4	1040	450	283	
B5				10.4	1040	450	283	

Note: L = length of the brace member without cruciform part; B = width; t = thickness; A = sectional area; λ = slenderness ratio on weak axis; P_y = yield axial load; δ_y = yield displacement in the axial direction.

Table 2 Material constants of brace members

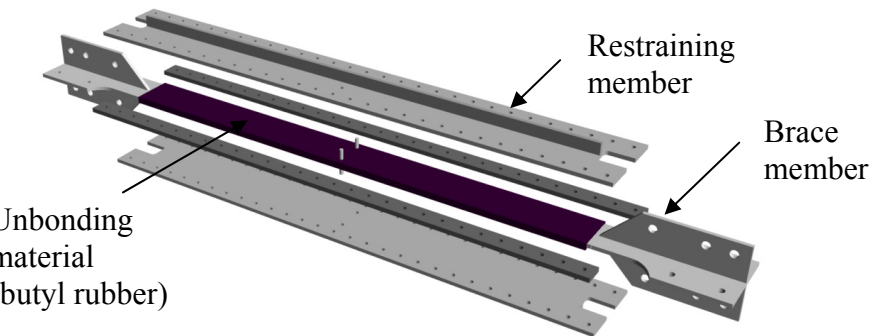
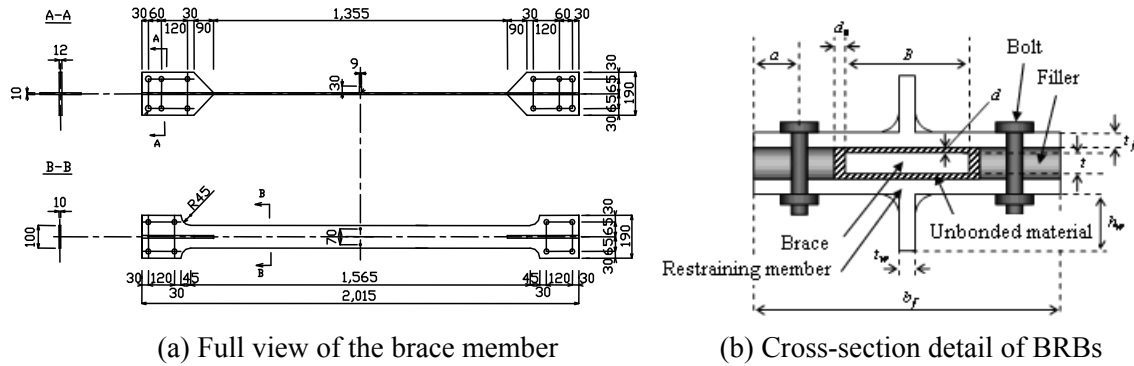
Specimens	E (GPa)	σ_y (MPa)	ε_y (%)	E_{st} (GPa)	ε_{st} (%)	σ_u (MPa)	ν
B1-B5	212	272	0.128	3.26	1.51	429	0.307

Note: E = Young's modulus; σ_y = yield stress; ε_y = yield strain; E_{st} = initial strain hardening modulus; ε_{st} = strain at onset of strain hardening; σ_u = tensile strength; ν = Poisson ratio.

Table 3 Geometric dimensions and structural properties of restraining members

Specimens	b_f (mm)	t_f (mm)	h_w (mm)	t_w (mm)	σ_y^R (MPa)	E^R (MPa)	Gap width(mm)	
							Out-plane d	In-plane d_0
B1		10.3	0	0			1	1
B2		10.4	19.7	10.4			1	1
B3	200	10.3	29.9	10.4	272	212	1	1
B4		10.3	39.8	10.3			1	4
B5		10.3	39.6	10.3			1	6

Note: Notations of b_f , t_f , h_w and t_w refer to Fig.2. σ_y^R = yield stress; E^R = Young's modulus.



(c) Assembly of BRB

Fig. 1 Configuration of the buckling restrained brace

(2) Restraining member

Fig. 1(b) shows the cross section detail of the BRB. Geometric dimensions and structural properties of the restraining member are listed in Table 3. The same SM400A mild steel is used for the restraining member. The web of the restraining member is made of a flat steel plate and the flange of the restraining member is welded to the web. In specimen of B1, plate shape restraining members, instead of T shape, are used, and h_w and t_w are zero as shown in Table 3. As shown later, to investigate the safety factor condition equation of Eq. (6), the safety factor ν_F of specimens of B1 and B2 are below 3.0 and the specimens of B3 to B5 are designed by $\nu_F > 3.0$.

(3) Unbonded material

The unbonded material is a kind of isolation material between the brace member and the restraining member that let the brace deform smoothly in the axial direction. In the tests, 1mm thick butyl rubber tape is bonded surrounding to the brace member as unbonded material.

(4) BRB assembly

The assembly of the BRB is shown in Fig. 1(c). First of all, the unbonded material is bonded to the brace member, then the brace member is installed between a pair of restraining members, and the restraining members are connected by high strength bolts.

BRB test setup. Fig. 2 shows the test setup. The specimen is horizontally pinned by high strength bolts between two rigid pillars and the brace member is horizontally placed. Two jacks are parallelly arranged in vertical direction and the loading is applied synchronously. The edge of specimens is treated to avoid eccentric axis load. Before installing specimens, initial deflection of the specimen in the direction perpendicular to plate plane of the brace member is measured and the specimen is installed so that the initial deflection directs downward.

Loading patterns. In the tests, a gradually increased tension and compression alternative cyclic loading is controlled by the axial displacement of specimens. In the tests of specimens B1, B3 and B4, the loading pattern began at $0.5\delta_y$, then increased with the increment of $1\delta_y$ from $1\delta_y$ to $6\delta_y$, with the increment of $2\delta_y$ from $6\delta_y$ to $12\delta_y$, and with the increment of $3\delta_y$ after $12\delta_y$. The loading was applied till final displacement of $24\delta_y$, which is defined as target performance at about strain of 3% in specimens. Moreover, considering the capacity limitation of the appliance and the contact influence between the restraining member and the cruciform section part of the brace member, in the tests of specimens of B3 and B4, several tension compression alternative cyclic loadings with the displacement of $18\delta_y$ were applied after the loading reached at the final displacement of $24\delta_y$. In the tests of specimens B2 and B5, the alternative loading pattern began at $0.5\delta_y$, then increased with the increment of $1\delta_y$ from $1\delta_y$ to $6\delta_y$, with the increment of $2\delta_y$ after $6\delta_y$. The target performance was also $24\delta_y$, i.e. approximate 3% of the axial strain.

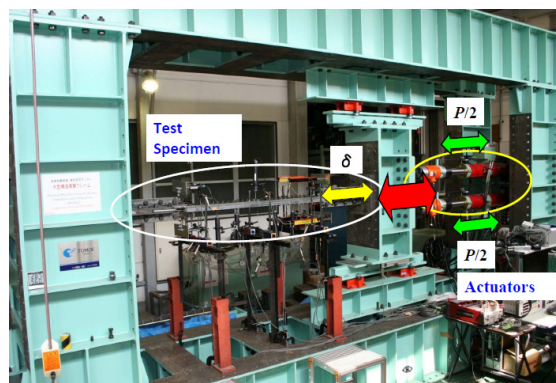


Fig. 2 Test setup

Analytical Model of BRBs

To compare with the test results, numerical analyses were also performed on cyclic behavior of BRBs with general finite element procedure ABAQUS by plane Timoshenko beam element of B21 considering shear deformation (ABAQUS,2006). The elasto-plastic model on overall buckling behavior of BRBs is presented as shown in Fig. 3, where half of a BRB is modeled

considering conditions of the symmetry. A pair of restraining members is simulated as two plane beams. To accurately simulate contact problem of deformation between the brace member and the restraining member, two plane beams are used for one brace member. The two plane beams of the brace member keep plane and are connected to each other by rigid elements, so as to the two plane beams for the restraining members.

The rigidity of unbonded material is neglected in the model because it has no influence on the brace member. However, when the unbonded material comes into contact with the restraining member in compression, friction effect exists between them. Thus the loading in the compression side is about 10% larger than that in the tension side and the static friction coefficient μ is in the model.

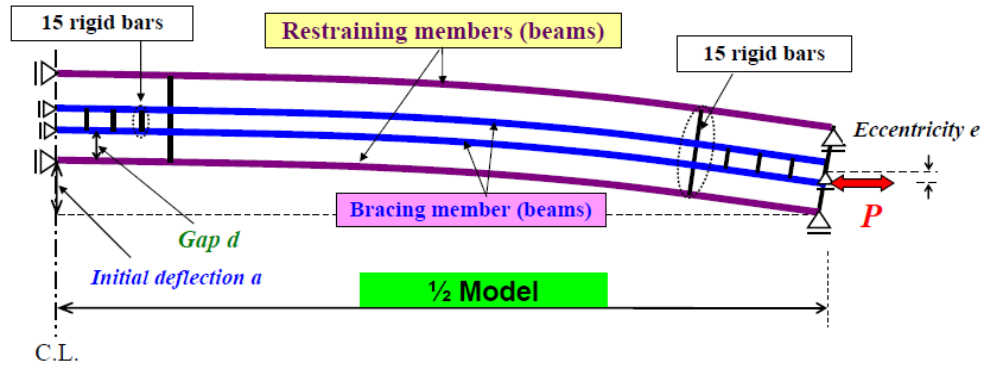


Fig. 3 The elasto-plastic model of BRBs

In the test specimens, the brace member and a pair of restraining members were all divided into 54 segments with equidistance. In the two beams of the brace and two beams for restraining members, nodes were connected to corresponding nodes by 15 rigid bars, respectively. Moreover, the freedom degree of Y was restrained the end node and freedom degrees of X and R_z were restrained at the node of the mid-span considering symmetry conditions.

Considering the initial state, the gap width between the brace member and the restraining member was constant and initial deflection of a sinusoidal pattern with maximum value of a was considered in the analysis. Moreover, in the direction of axial force, loading eccentricity of e was also considered in the model.

The modified two surface model (Shen et al. 1995) was used for the constitutive law in the analysis and material constants were $E = 206\text{GPa}$, $\sigma_y = 235\text{MPa}$, $\varepsilon_y = 0.00114$, $E_{st}/E = 1/40$, $\varepsilon_{st}/\varepsilon_y = 10$, and $\nu = 0.3$.

RESULTS AND COMPARISON

The relations of axial loading P/P_y to axial deformation δ/δ_y of all the specimens are shown in Fig. 4. The tensile state of BRBs is displayed in the positive direction, the axial loading P is normalized by yield axial force P_y in the longitudinal coordinate and the axial displacement δ is normalized by yield axial displacement δ_y in the abscissa. Test results are summarized in Table 4.

It is shown in the hysteretic curve of specimen of B1 that in the loading path from the tension side of $\delta/\delta_y=+6$ to the compression side of $\delta/\delta_y=-6$, the strength decreased rapidly near $\delta/\delta_y=-3$. Later, after reaching the loading at $\delta/\delta_y=-6$, the specimen of B1 was tensioned to $\delta/\delta_y=+7$, and then was compressed again, it is found that it became impossible for the loading beyond the

strength detected at $\delta/\delta_y = -3$ and unloading was applied when the axial displacement reached zero. It is concluded that overall buckling occurred in the BRB specimen of B1 near $\delta/\delta_y = -3$ and the strength deteriorated. Similar hysteretic curve can be found in the specimen of B2. In the compression loading path from $\delta/\delta_y = +18$ to $\delta/\delta_y = -18$, the strength decreased rapidly near $\delta/\delta_y = -14$. Later, after reaching the loading of $\delta/\delta_y = -18$, the specimen B2 was tensioned to $\delta/\delta_y = +18$, and then was compressed again, the loading also can not be applied to the strength detected at $\delta/\delta_y = -14$ and unloading was applied when the axial displacement reached zero. Photo 1 shows the overall buckling of the whole BRB member of B2. In the test of B3-B5, stable hysteretic curves were obtained without overall buckling occurrence in the whole loading history and the maximum strain exceeded the limit strain of 3%. From the test results listed in Table 5, it is also found that overall buckling occur before the limit strain and CID in the cases of B1 and B2 with $v_F < 3.0$. However, in the case of B3-B5, overall buckling did not occur with $v_F \geq 3.0$ and the maximum strain and CID all exceeds the limit value.

Table 4 Test results of BRBs

Specimens	$\left(\frac{P_E^R}{P_y}\right)_{no\ minal}$	$\left(\frac{M_y^R}{P_y L}\right)_{no\ minal}$	v_F	Overall buckling happen?	CID	ϵ_{max} (%)
B1	2.43	0.0239	2.06	Yes	0.05	0.78
B2	3.76	0.0164	2.69	Yes	0.22	2.31
B3	5.34	0.0183	3.54	No	>0.81	>3.08
B4	7.79	0.0219	4.81	No	>0.74	>3.07
B5	7.79	0.0219	4.81	No	>0.73	>3.06

Note: The safety factor v_F is calculated by Eq.(6) with $a=L/1000$, $d=1\text{mm}$ and $e=0.0$.

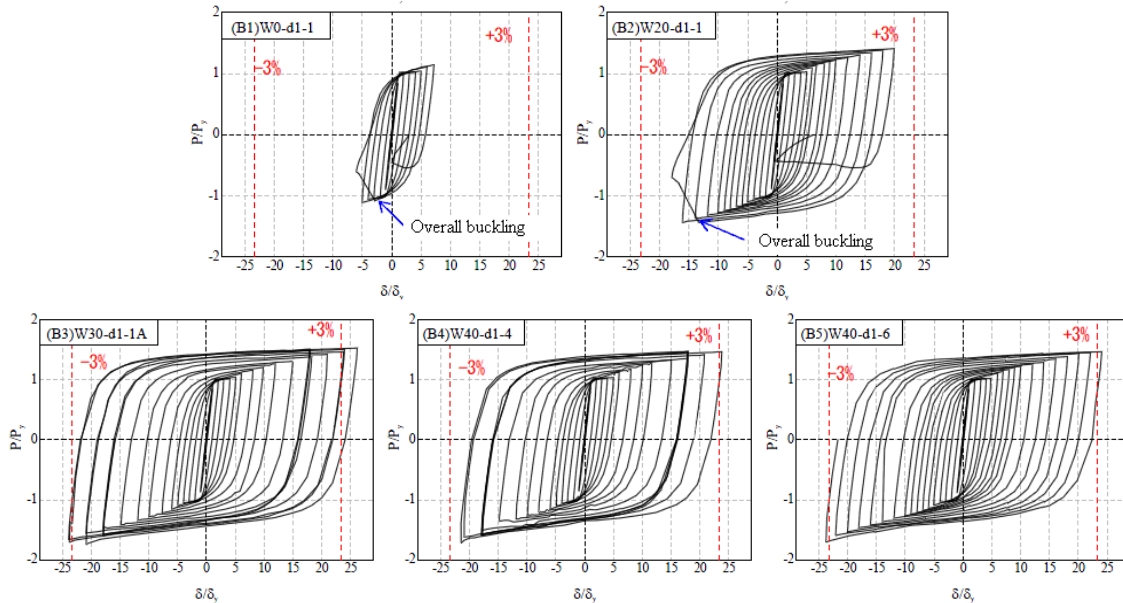


Fig. 4 Experimental Loading-displacement relationship in the axial direction



Photo 1 Over-all buckling failure in BRB specimen of B2

Fig.5 shows a comparison of the test result and analytical result. The specimens of B2 and B5 were analyzed by the elasto-plastic model mentioned in the above section. As shown in Fig. 5(a), in the analysis of B2, static friction coefficient of 0.075 was considered for the contact influence between the unbonded material and the restraining member and small eccentricity of 1.8mm in the axial direction was also considered. As shown in Fig. 5(b), the numerical analyses with and without friction influence were both carried out. It is found that the analytical results agree well with the test ones in both cases. Therefore, it can be concluded that the proposed model can accurately simulate the cyclic behavior of high performance BRBs.

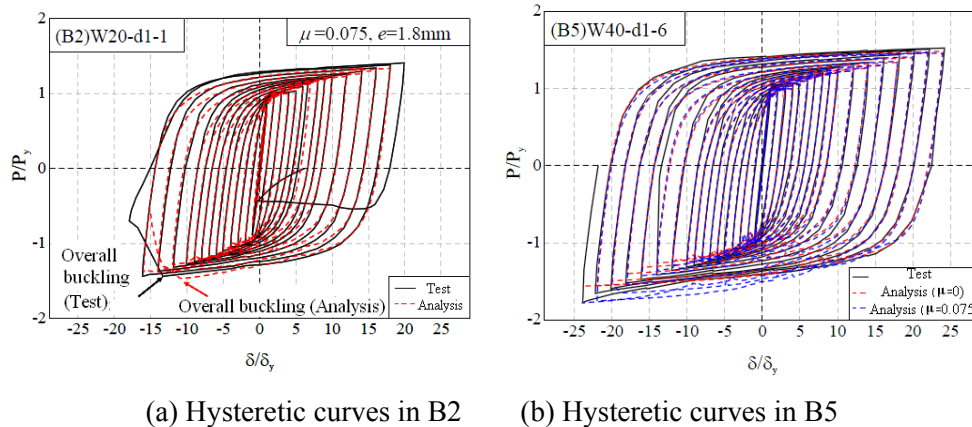


Fig. 5 Results comparison between tests and analyses

From comparison of test results and analysis, it can be concluded that $v_F \geq 3.0$ is a sufficient condition for the prevention of overall buckling of BRBs, and BRBs without overall buckling fulfill the requirement of high performance dampers.

CONCLUSIONS AND RESEARCH NEEDS

In the paper, the performance requirements of HPSDs were proposed. A type of steel hysteretic damper, i.e. the buckling restrained brace, was experimental and analytical studied to investigate the applicability of HPSDs. Conclusions can be drawn as follows:

- (1) Overall buckling would not occur for BRBs with $v_F \geq 3.0$ and BRBs without overall buckling fulfill the HPSD's target performances. Also, BRBs with $v_F \geq 3.0$ agree with the target performance of HPSD.

- (2) The proposed elasto-plastic model can successfully simulate the behavior of BRBs even with overall buckling.

Some research needs are presented due to the above discussions:

- (1) Design method for gusset plate and surrounding parts need to be proposed.
- (2) Smart material application for seismic dampers, such as aluminum alloy and shape memory alloy seems necessary to be studied.
- (3) Effectiveness of using seismic dampers and their optimal placement in bridges should be researched.
- (4) Verification of seismic dampers' effectiveness should be carried out by shaking table tests.

ACKNOWLEDGEMENT

The study was supported in part by grants from the Advanced Research Center for Seismic Experiments and Computations, Meijo University.

REFERENCES

- Lai, J.W. and Tsai, K.C. 2004. Research and application of buckling restrained braces in Taiwan, *ANCER Annual Meeting 2004*, Hawaii, USA.
- ABAQUS. 2006. *Analysis User's Manual (version 6.6)*. ABAQUS, Inc., Pawtucket, R.I.
- Shen, C., Mamaghani, I.H.P., Mizuno, E. and Usami, T. 1995. Cyclic behavior of structural steels: theory. *Journal of Engineering Mechanics*, ASCE, 121(11), pp. 1165-1172.
- Usami, T., Lu, Z., Ge, H.B. 2005. A seismic upgrading method for steel arch bridges using buckling-restrained braces, *Earthquake Engineering and Structural Dynamics*, Vol. 34, pp. 471-496,
- Iwata, M. and Murai, M. 2006. Buckling-restrained brace using mortal planks: performance evaluation as a hysteretic damper, *Earthquake Engineering and Structural Dynamics*, Vol. 35, pp. 1807-1826,
- Carden, L.P., Itani, A.M. and Buckle, L.G. 2006. Seismic performance of steel girder bridges with ductile cross frames using buckling-restrained braces. *Journal of Structure Engineering*, ASCE, 132(3), pp. 338-345.
- Weber, F., Feltrin, G. and Huth, O. 2006. *Guidelines for structural control*. Structural Engineering Research Laboratory, Swiss Federal Laboratories for Material Testing and Research, Dubendorf, Switzerland.
- Fahnestock, L.A, Sause, R. and Ricles, J.M. 2007. Seismic Response and Performance of Buckling-Restrained Braced Frames, *Journal of Structure Engineering*, ASCE, 133(9), pp. 1195-1204.
- Fahnestock, L.A., Ricles, J.M. and Sause, R. 2007. Experimental Evaluation of a Large-scale Buckling-Restrained Braced Frame, *Journal of Structure Engineering*, ASCE, 133(9), pp. 1205-1214.
- Usami, T. 2007. Developing high-performance damage control seismic dampers. *Proceedings of the 10th symposium on ductile design method for bridges (Special Lecture)*, JSCE, pp. 11-22.(in Japanese)
- Uriz, P and Mahin, S.A. 2008. *Toward earthquake-resistant design of concentrically braced steel-frame structures*. PEER Report 2008/08. Pacific Earthquake Engineering Research Center, Berkeley, Calif.

- Usami, T., Ge, H.B. and Kasai, K. 2008: Overall Buckling Prevention Condition of Buckling-Restrained Braces as a Structural Control Damper, Proc. the 14th World Conference on Earthquake Engineering, Beijing, China.
- Andrews, B.M., Fahnestock, L.A. and Song, J. 2009. Ductility capacity models for buckling-restrained braces, *Journal of Constructional Steel Research*, ASCE, 65, pp. 1712-1720.
- Celik, O. and Bruneau, M. 2009. Seismic behavior of bidirectional-resistant ductile end diaphragms with buckling restrained braces in straight steel bridges. *Engineering Structures*, 31, pp.380-393.
- Usami, T., Sato, T. and Kasai, A. 2009. Developing high-performance buckling restrained braces. *Journal of Structural Engineering*, JSCE, 55A, pp. 719-729.(in Japanese)